

Cat Codes with Optimal Decoherence Suppression for a Lossy Bosonic Channel

Linshu Li,¹ Chang-Ling Zou,¹ Victor V. Albert,¹ Sreeram Muralidharan,² S. M. Girvin,¹ and Liang Jiang¹

¹*Departments of Applied Physics and Physics, Yale University, New Haven, Connecticut 06511, USA*

²*Department of Electrical Engineering, Yale University, New Haven, Connecticut 06511, USA*

(Received 29 September 2016; published 21 July 2017)

We investigate cat codes that can correct multiple excitation losses and identify two types of logical errors: bit-flip errors due to excessive excitation loss and dephasing errors due to quantum backaction from the environment. We show that selected choices of logical subspace and coherent amplitude significantly reduce dephasing errors. The trade-off between the two major errors enables optimized performance of cat codes in terms of minimized decoherence. With high coupling efficiency, we show that one-way quantum repeaters with cat codes feature a boosted secure communication rate per mode when compared to conventional encoding schemes, showcasing the promising potential of quantum information processing with continuous variable quantum codes.

DOI: 10.1103/PhysRevLett.119.030502

An outstanding challenge for quantum information processing with bosonic systems is excitation loss, which can be modeled as a lossy bosonic channel (LBC) [1,2]. To suppress excitation loss, conventionally the approach is to consider discrete variable (DV) encodings [3–8] that use physical qubits (qudits) realized with a single excitation distributed over two (multiple) bosonic modes and standard qubit- (qudit-) based quantum error correction (QEC). Such DV encoding schemes usually require a considerable number of bosonic modes to encode one logical qubit (qudit). In contrast, continuous variable (CV) encoding schemes deploy the Hilbert space of higher excitations, enabling single-mode based QEC against loss errors. The resulting mode efficiency can potentially lead to high-storage-density quantum memories and boost the secure communication rate per mode for long-distance quantum communication [9–15].

Cat codes [2,16,17], among other single-mode CV schemes [18,19], have been proposed for correcting excitation loss. With the rapid development of quantum control [20–22] and high-fidelity quantum nondemolition readout [23–25], QEC with cat codes has recently been demonstrated to reach the break-even point in superconducting circuits [26]. These advances have opened up a new era of CV quantum information in which states can be stored and manipulated for a duration longer than the intrinsic coherence time of the constituent modes.

Cat codes are based on superpositions of coherent states. Qualitatively it is known that a proper choice of coherent amplitude α is essential for their QEC performance: a large α increases the probability of uncorrectable excitation loss while a small α leads to significant overlap between neighboring coherent components. Yet, to date, the optimal choice of α and, hence, the optimal QEC capability of cat codes have remained unquantified. In this Letter, we investigate cat codes that encode a logical qubit in superpositions of $2d$ ($d \geq 2$) coherent components and can correct up to $d - 1$ excitation losses [16,17]. We quantify the two major

types of errors associated with the encoding: **the logical bit-flip error due to finite capability of correcting losses, and the logical dephasing error induced by backaction from the environment.** The analysis reveals nontrivial choices of code parameters that significantly reduce the backaction and balance the two logical errors. Using parameters yielding minimum decoherence, we analyze the performance of cat codes in one-way quantum repeaters (QRs) for ultrafast quantum communication over transcontinental scales.

Lossy bosonic channel.—The Kraus operator-sum representation for the LBC is [1]

$$\mathcal{L}(\rho) = \sum_{k=0}^{\infty} E_k \rho E_k^\dagger, \quad (1)$$

where $E_k = (1/\sqrt{k!})\gamma^{k/2}(1-\gamma)^{a^\dagger a/2}a^k$ is the Kraus operator associated with losing k excitations, a (a^\dagger) is the annihilation (creation) operator, and γ is the loss probability of each excitation. Excitation loss in bosonic systems, such as localized cavity modes for quantum memories and propagating modes for quantum communication, can be modeled as a LBC. For cavities, $\gamma = 1 - e^{-\kappa t}$, where κ is the cavity decay rate and t is the storage time; for propagating modes with attenuation length L_{att} , $\gamma = 1 - \eta^2 e^{-L/L_{\text{att}}}$, where L is the propagation distance and η is the coupling efficiency of the interface between the optical channel and local processing devices.

Cat codes and properties.—The basis states of cat codes are defined as superpositions of $2d$ coherent states lying equidistantly on a circle in the phase space of a bosonic mode,

$$\begin{aligned} |C_\alpha^n\rangle &= \frac{1}{2d\sqrt{N_\alpha^n}} \sum_{k=0}^{2d-1} \omega^{-kn} |\omega^k \alpha\rangle \\ &= \frac{1}{\sqrt{N_\alpha^n}} \sum_{m=0}^{\infty} \frac{e^{-1/2|\alpha|^2} \alpha^{n+2md}}{\sqrt{(n+2md)!}} |n+2md\rangle_F, \end{aligned} \quad (2)$$

where $\omega = e^{i\pi/d}$, $|l\rangle_F$ is the Fock state with l excitations, and $n = 0, 1, 2, \dots, 2d-1$ uniquely labels the $2d$ basis states. The normalization factor reads [27,28]

$$N_\alpha^n = \frac{1}{2d} \sum_{k=0}^{2d-1} e^{(\omega^k-1)\alpha^2/\omega^{kn}} = \sum_{m=0}^{\infty} |\langle \alpha | n + 2md \rangle_F|^2. \quad (3)$$

Without losing generality, we assume α is real and positive. Since $|C_\alpha^n\rangle$ is a superposition of $n \bmod 2d$ Fock states ($|n\rangle_F$, $|n+2d\rangle_F$, $|n+4d\rangle_F$, ...), cat states are orthonormal, $\langle C_\alpha^n | C_\alpha^m \rangle = \delta_{nm}$. The average excitation number $\langle a^\dagger a \rangle_n = \alpha^2 N_\alpha^{n-1} / N_\alpha^n \rightarrow \alpha^2$ for $\alpha \rightarrow \infty$ [29], as shown in Fig. 1(b), while for finite α it deviates from α^2 due to the oscillatory $N_\alpha^{n-1} / N_\alpha^n$.

The $2d$ -dimensional cat Hilbert space can be divided into d subspaces labeled by $s = 0, 1, \dots, d-1$. The “ s subspace” has excitation number $s \bmod d$, spanned by two logical states $|0_L\rangle^s = |C_\alpha^s\rangle$ and $|1_L\rangle^s = |C_\alpha^{s+d}\rangle$. Figure 1(a) shows the Wigner functions and excitation distributions of $|C_\alpha^s\rangle$ and $|C_\alpha^{s+d}\rangle$ for $d = 3$, $\alpha = 3$, and $s = 0$. It becomes clear that d , α , and s are three degrees of freedom that determine the performance of cat codes in protecting quantum states against LBCs.

After losing k excitations, the s subspace is mapped to the $(s-k)$ subspace, $|C_\alpha^s\rangle \rightarrow |C_\alpha^{s-k}\rangle$ and $|C_\alpha^{s+d}\rangle \rightarrow |C_\alpha^{s+d-k}\rangle$. Hence, we can unambiguously distinguish $0 \leq k \leq d-1$ losses without destroying the encoded logical states by projectively measuring the excitation number mod d (called the “ \mathbb{Z}_d measurement”). In fact, since a cat state maps back to itself after losing integer multiples of $2d$ excitations, we can restore the logical states correctly with $2md \leq k \leq (2m+1)d-1$ losses for integer m . If there are $(2m+1)d \leq k \leq 2(m+1)d-1$ losses, however, we will misidentify the

logical states. Since the symmetric superposition $|C_\alpha^s\rangle + |C_\alpha^{s+d}\rangle \rightarrow |C_\alpha^{s-k}\rangle + |C_\alpha^{s+d-k}\rangle$ is preserved even if we misidentify the logical states, the misidentification effectively induces an X rotation in the logical basis—a logical bit-flip error.

In addition to the logical bit-flip error, the LBC can induce another type of error via environment backaction resulting from nonzero overlap between neighboring coherent components. For finite α , the logical states $|C_\alpha^s\rangle$ and $|C_\alpha^{s+d}\rangle$ generically differ in average excitation number, as shown in Fig. 1(b), as well as the m th moments $\langle (a^\dagger a)^m \rangle_s \neq \langle (a^\dagger a)^m \rangle_{s+d}$ for $m \in \mathbb{Z}^+$. Hence, the excitation loss to the environment leaks out information about the encoded state, which is captured by Kraus operators acting on logical states, $E_k |C_\alpha^n\rangle \propto (1-\gamma)^{a^\dagger a/2} a^k |C_\alpha^n\rangle = e^{-\Delta} \alpha^k \sqrt{N_\alpha^{n-k}/N_\alpha^n} |C_\alpha^{n-k}\rangle$ with $\alpha' = \sqrt{1-\gamma}\alpha$ and $\Delta = \gamma\alpha^2$. The fact that $N_\alpha^{n-k}/N_\alpha^n$ is slightly different for $n = s$ and $n = s+d$ results in a backaction associated with losing k excitations [35]. Though when we average over all possible k , the backaction-induced bias towards $|C_\alpha^s\rangle$ or $|C_\alpha^{s+d}\rangle$ is mostly canceled, the backaction does reduce the coherence between $|C_\alpha^s\rangle$ and $|C_\alpha^{s+d}\rangle$ and effectively induces a logical dephasing error.

QEC recovery for cat codes.—Consider encoding with a fixed $s \in \{0, 1, \dots, d-1\}$. To protect the quantum information from bosonic loss, we introduce a QEC recovery operation \mathcal{R} [Fig. 1(d)], which consists of a \mathbb{Z}_d measurement, conditional loss compensation, and amplitude restoration. First, we use the \mathbb{Z}_d measurement to distinguish different loss events up to losing $d-1$ excitations. Similar to the qubit-assisted parity (\mathbb{Z}_2) measurement [25], we consider a d -level ancilla (e.g., using higher levels of a transmon [36]) that couples to a cavity via a dispersive Hamiltonian $H_{DC} = \sum_{j=0}^{d-1} j\chi |j\rangle\langle j| a^\dagger a$, where $|j\rangle$ are the basis states of the ancilla. Combined with Fourier gates on the ancilla, F_d , we can implement the unitary operation

$$U_{DC} = F_d^\dagger e^{-i(\pi/\chi)H_{DC}} F_d, \quad (4)$$

which maps the \mathbb{Z}_d information to the ancilla that is subsequently measured in $\{|j\rangle\}$ basis. Then, conditioned on the loss rate γ and measured excitation loss number (mod d), $k \in \{0, 1, \dots, d-1\}$, we implement the following unitary to restore the state back to the s subspace:

$$U_k = (|C_\alpha^s\rangle\langle C_\alpha^{s-k}| + |C_\alpha^{s+d}\rangle\langle C_\alpha^{s+d-k}| + \text{H.c.}) + U_k^0, \quad (5)$$

where U_k^0 is an arbitrary unitary on the complementary subspace of $\text{span}\{|C_\alpha^s\rangle, |C_\alpha^{s+d}\rangle, |C_\alpha^{s-k}\rangle, |C_\alpha^{s+d-k}\rangle\}$, so that U_k is a unitary on the entire Hilbert space. Finally, we restore the amplitude via the following unitary:

$$S = |C_\alpha^s\rangle\langle C_\alpha^s| + |C_\alpha^{s+d}\rangle\langle C_\alpha^{s+d}| + S^0, \quad (6)$$

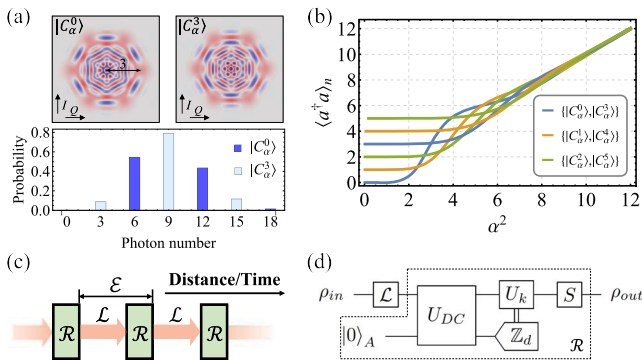


FIG. 1. (a) Wigner functions and excitation number distributions of $|C_3^0\rangle$ and $|C_3^3\rangle$ with $d = 3$. (b) Average excitation number $\langle a^\dagger a \rangle_n$ for cat states with $d = 3$. (c) Schematic of alternating LBC (\mathcal{L}) and QEC recovery (\mathcal{R}). (d) Quantum circuits of QEC recovery for cat codes, consisting of the dispersive coupling gate U_{DC} followed by \mathbb{Z}_d measurement of excitation number, conditional rotation gate U_k compensating the lost excitations, and, finally, amplitude restoration S .

where S^0 is a complementary operation that makes S a unitary on the entire Hilbert space. Using Eq. (2), we can express U_k and S in the Fock basis and realize them using SNAP gates [20] or gradient ascent pulse engineering [37], as recently demonstrated in dispersively coupled superconducting transmon-cavity systems [21,22]. For S , alternatively, we may also use engineered dissipation to restore the amplitude [17,38]. Overall, the QEC recovery in Fig. 1(d) implements

$$\mathcal{R}(\rho) = \sum_{k=0}^{d-1} |C_\alpha^s\rangle \langle C_\alpha^{s-k} | \rho | C_\alpha^{s-k}\rangle \langle C_\alpha^s|, \quad (7)$$

which restores the original encoded subspace. Note that the QEC recovery \mathcal{R} with Kraus rank d can also be implemented using a two-level ancilla, with $\lceil \log_2 d \rceil$ steps of measurement and feedforward control [39,40].

Logical bit-flip and dephasing errors.—In the regime where (i) the probability of misidentifying logical states due to excessive loss and (ii) the overlap between neighboring coherent states in the superpositions are small, we can approximate $\mathcal{E} = \mathcal{R} \circ \mathcal{L}$ as a Pauli channel [29],

$$\mathcal{E}(\rho) \approx (1 - \epsilon_f - \epsilon_d)\rho + \epsilon_f X\rho X + \epsilon_d Z\rho Z, \quad (8)$$

where logical bit-flip error ϵ_f and logical dephasing error ϵ_d are

$$\epsilon_f = \sum_{k=d}^{2d-1} \sum_{m=0}^{\infty} \frac{e^{-\Delta} \Delta^{2md+k}}{(2md+k)!}, \quad (9)$$

$$\epsilon_d = \frac{e^{4\Delta \sin^2(\pi/2d)} - \sqrt{1 - 2e^\mu \cos \psi + e^{2\mu} \cos \theta} - 1}{2e^{4\alpha^2 \sin^2(\pi/2d)}}, \quad (10)$$

where $\mu = 2\Delta(2\sin^2[\pi/2d] - \sin^2(\pi/d))$, $\psi = \Delta[2\sin(\pi/d) - \sin(2\pi/d)]$, $\theta = 2s\pi/d - 2\alpha^2 \sin(\pi/d) - \tan^{-1}[e^\mu \sin \psi / (1 - e^\mu \cos \psi)]$. To quantify the residual decoherence after \mathcal{R} , we consider the effective error rate $\Gamma(\alpha, d, \gamma, s) \triangleq \frac{1}{2} \|\mathcal{E} - \mathcal{I}\|_\diamond$, where \mathcal{I} is the identity channel and $\frac{1}{2} \|\cdot\|_\diamond$ is the diamond distance [41,42]. For small errors, $\Gamma \approx \epsilon_f + \epsilon_d$ (see details in [29]).

For given γ and d , we may select coherent amplitude α and logical subspace s to minimize Γ . As illustrated in Fig. 2, for each fixed s -subspace encoding, the Γ oscillates with α^2 and there is a set of α where the dephasing is suppressed to second order, reaching local minima [29]. In fact, each dip corresponds to an α at which $\langle a^\dagger a \rangle_s = \langle a^\dagger a \rangle_{s+d}$ [associated with the crossing points in Fig. 1(b)] and the residual backaction only comes from the difference in higher moments of $a^\dagger a$.

To estimate the range of Γ , we can analytically express the approximate upper and lower bounds

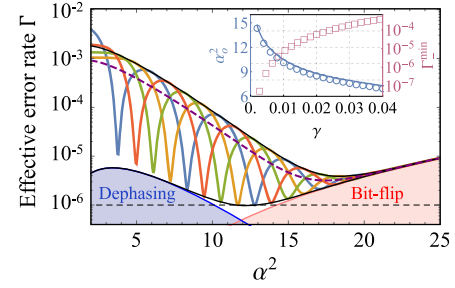


FIG. 2. Effective error rate (numerical) for logical subspace $s = 0, 1, 2, 3$ (blue, red, green, and orange solid curves, respectively) and analytical bounds Γ_\pm from Eq. (11) (black solid), for $d = 4$ and $\gamma = 0.5\%$. The two types of errors in Γ_- , logical bit-flip error ϵ_f and dephasing error $\epsilon_d|_{\cos\theta=1}$, are shown. The purple and black dashed lines mark $\bar{\Gamma}$ and the minimized decoherence Γ_-^{\min} , respectively. The inset shows the dependence of Γ_-^{\min} and α_0^2 on γ . The approximate α_0^2 from Eq. (12) (solid line) agrees well with numerics.

$$\Gamma_\pm(\alpha, \gamma, d) = \epsilon_f + \epsilon_d|_{\cos\theta=\mp 1}. \quad (11)$$

As illustrated in Fig. 2, to reach the minimum Γ_- (lower black curve), it is crucial to perform combined optimization of α and s . In fact, if we are nonselective in the logical subspace (i.e., averaging over all s) and only optimize the coherent amplitude α , the averaged error rate $\bar{\Gamma} = \frac{1}{2}(\Gamma_+ + \Gamma_-) \approx \frac{1}{2}\Gamma_+$ (dashed purple curve) can be orders of magnitude larger than Γ_- for the parameter region of interest. Moreover, the combined optimization notably leads to a smaller optimized coherent amplitude.

We can estimate the optimal amplitude α_0 that minimizes Γ_- by equating the two errors in Eq. (11). For $\Delta \ll d$, we have

$$\alpha_0^2 \approx \xi W(\sqrt{\pi^A d! / 2d^A} / \xi \gamma) \quad (12)$$

for $d > 2$, where $\xi = (d-2)/[4\sin^2(\pi/2d) - \gamma]$ and W is the Lambert W function $z = f^{-1}(ze^z) = W(ze^z)$. The inset of Fig. 2 shows that Eq. (12) reasonably approximates the exact α_0 . Based on the estimated α_0 , we can identify the best combination of α^* and s^* near the vicinity of Γ_-^{\min} .

Application to repetitive correction.—So far we have considered the optimization of cat codes for one round of LBC followed by QEC recovery, and identified the optimal amplitude α and logical subspace s for given d and γ . For practical applications, however, repetitive correction can be needed. In the following, we consider one-way QRs [14,15,43,44] with cat codes over transcontinental distances ($\geq 10^3$ km) and optimize repeater spacing L_0 to best maintain the coherence.

Introducing the dimensionless repeater spacing $\tilde{L}_0 = L_0/L_{\text{att}}$ ($L_{\text{att}} = 20$ km for optical fiber), we notice that typically $\tilde{L}_0 \ll 1$ for one-way QRs, so that the fiber-induced loss is correctable. The goal is to minimize the error accumulation rate

$$\tau_-(\alpha, \tilde{L}_0, d) = \Gamma_-(\alpha, \gamma, d)/\tilde{L}_0. \quad (13)$$

Figure 3(a) shows the minimized τ_- as a function of d for $\eta = 99.5\%$ with the associated arc length between neighboring coherent states $\pi\alpha_{\text{opt}}/d$. We observe that the minimized τ_- is anticorrelated with $\pi\alpha_{\text{opt}}/d$, as an increasing arc length reduces the coherent component overlap and consequently suppresses the dephasing. For small d , the overall bit-flip error is better suppressed as d increases, thus favoring a larger arc length; for large d , however, the typical number of losses roughly is $\Delta \propto \gamma d^2$, leading to fast-growing uncorrectable loss errors. Hence, there is an optimized choice of d that minimizes the overall error.

For one-way QRs with cat codes, the quantum operation of the chain [Fig. 1(c)] can be modeled by $\mathcal{E}^N = (R \circ \mathcal{L})^N$, with $N = L_{\text{tot}}/\tilde{L}_0^{\text{opt}} L_{\text{att}}$ stations, and we consider quantum key distribution to evaluate the performance [29]. Using the optimized secure key rate per mode (SKRPM) as a metric, in Fig. 3(b) we compare the performance of one-way QRs [47] with cat codes, quantum parity code (QPC) [15,46], and quantum polynomial code (QPyC) [45] for $\eta = 99.5\%$. We see that, with high coupling efficiency, cat codes make better use of the mode resource and can achieve much higher SKRPM over thousands of kilometers compared with DV quantum codes.

Discussion on imperfections.—So far, we have only considered suppressing decoherence induced by photon loss. Nonetheless, QEC recovery [Fig. 1(d)] in practice can be faulty. To achieve a comparable performance enhancement (from $\bar{\Gamma}$ to Γ_-) as the ideal case, the error introduced by recovery should be sufficiently small $\epsilon_{\text{rec}} \lesssim \Gamma_-$. As detailed in the Supplemental Material [29], various imperfections can be efficiently suppressed. The dominant imperfection is the T_1 decay of the ancilla during dispersive coupling, which may lead to unreliable \mathbb{Z}_d measurement and an imperfect U_k gate. Besides experimentally improving the T_1 time of the ancilla [48–50], there are various approaches to suppress the errors induced by the

ancilla decay. For example, we may use resonant coupling between the ancilla and the cavity for faster quantum gates, with gate time (~ 10 ns [51,52]) much shorter than that for dispersive coupling (~ 1 μ s [22]) and, consequently, suppress the error from the ancilla decay.

Alternatively, we may implement an equivalent recovery circuit without suffering from ancilla decay. It contains three modifications: (i) use majority voting based on repeated parity measurement and dispersion engineering to suppress the measurement error due to ancilla decay to higher order, (ii) switch the logical subspace to the $(s - k)$ subspace to avoid the U_k gate, and (iii) for amplitude restoration S , restore α to the value that is close to the optimal amplitude α_0 and minimizes $\Gamma(\alpha, d, \gamma, s - k)$. As the variation in Γ_- is small near α_0 , switching to $(s - k)$ subspace can still achieve a small effective error rate. We note S can be achieved via multiphoton pumping [17] insensitive to ancilla decay as it only virtually excites the ancilla. Therefore, the modified circuit can be robust against ancilla decay and other imperfections [29].

Conclusion and outlook.—We have investigated cat codes for protecting quantum states against bosonic excitation loss. At the encoded level, there are two major types of uncorrectable errors, logical bit-flip error due to excessive excitation loss and logical dephasing error induced by backaction. We have demonstrated that the nontrivial combination of coherent amplitude and logical subspace can efficiently suppress logical dephasing error and lead to greatly improved quantum error correction performance. We expect to observe suppressed backaction in other approximate continuous variable quantum codes as $\langle 0_L | a^\dagger a | 0_L \rangle = \langle 1_L | a^\dagger a | 1_L \rangle$ is satisfied and the balance between the backaction and excessive excitation loss is critical for optimizing their performances. Comparison between cat codes and other single-mode schemes, such as the Gottesman, Kitaev, and Preskill codes [18,53,54] and binomial codes [19], over a lossy bosonic channel could shed light on the optimal construction of single-mode quantum code. We notice that cat codes become less favorable than conventional multimode schemes in the case of long communication distance [Fig. 3(b)] and/or high coupling loss [29], as a result of high occupation of a single mode. This will motivate us to explore unconventional multimode continuous variable encodings with multiple excitations per mode [55] that may asymptotically achieve the channel capacity of a lossy bosonic channel.

As an application, we have explored one-way quantum communication over long distances with cat codes and found that, given high-fidelity coupling into and out of the repeaters, this single-mode scheme can outperform conventional ones with a single excitation occupying multiple modes, in terms of secure key rate per mode. Such cat encoding of flying qubits can also be used for remote entanglement generation with error correction [56] and quantum state transfer via noisy photonic or phononic

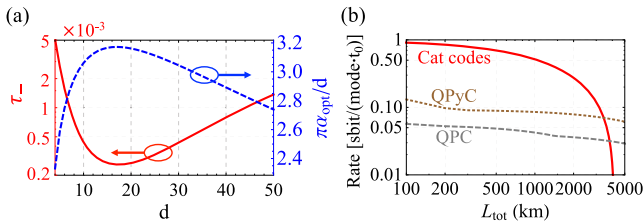


FIG. 3. Optimized performance of cat codes for QRs with $\eta = 99.5\%$ and comparison with selected DV schemes. (a) Minimum error accumulation rate τ_- (red) and associated optimum arc length $\pi\alpha_{\text{opt}}/d$ (blue). (b) Optimized SKRPM over long distances for one-way QRs with cat codes (red solid), quantum polynomial codes [45] (brown dotted), and quantum parity codes [15,46] (gray dashed). t_0 is the gate operation time taken as the same for three schemes.

waveguides [57,58]. With recent progress on efficient coupling between fiber and optical waveguides [59], and high-fidelity frequency conversion between optical and microwave modes [60–62], we may even envision realistic quantum repeaters consisting of superconducting circuits for error correction and optical-microwave quantum transducers for protecting transmitted quantum information against photon loss in optical channels.

We thank Kasper Duivenvoorden, Jungsang Kim, Norbert Lütkenhaus, Marios H. Michael, Ananda Roy, Chao Shen, Barbara Terhal, and Hong Tang for stimulating discussions. We acknowledge support from the ARL-CDQI, ARO (Grants No. W911NF-14-1-0011 and No. W911NF-14-1-0563), ARO MURI (Grant No. W911NF-16-1-0349), NSF (Grants No. DMR-1609326 and No. DGE-1122492), AFOSR MURI (Grants No. FA9550-14-1-0052 and No. FA9550-15-1-0015), the Alfred P. Sloan Foundation (Grant No. BR2013-049), and the Packard Foundation (Grant No. 2013-39273).

Note added.—The authors recently became aware of a related work on cat codes [63]. Different from that work, here we propose a deterministic amplitude restoration for recovery and consider combined optimization of amplitude and logical subspace.

-
- [1] I. L. Chuang, D. W. Leung, and Y. Yamamoto, *Phys. Rev. A* **56**, 1114 (1997).
 - [2] P. T. Cochrane, G. J. Milburn, and W. J. Munro, *Phys. Rev. A* **59**, 2631 (1999).
 - [3] T. C. Ralph, A. J. F. Hayes, and A. Gilchrist, *Phys. Rev. Lett.* **95**, 100501 (2005).
 - [4] C. M. Dawson, H. L. Haselgrove, and M. A. Nielsen, *Phys. Rev. Lett.* **96**, 020501 (2006).
 - [5] M. Varnava, D. E. Browne, and T. Rudolph, *Phys. Rev. Lett.* **97**, 120501 (2006).
 - [6] M. Varnava, D. E. Browne, and T. Rudolph, *New J. Phys.* **9**, 203 (2007).
 - [7] S. D. Barrett and T. M. Stace, *Phys. Rev. Lett.* **105**, 200502 (2010).
 - [8] Y. Li, S. D. Barrett, T. M. Stace, and S. C. Benjamin, *New J. Phys.* **15**, 023012 (2013).
 - [9] H.-K. Lo, M. Curty, and K. Tamaki, *Nat. Photonics* **8**, 595 (2014).
 - [10] M. Takeoka, S. Guha, and M. M. Wilde, *Nat. Commun.* **5**, 5235 (2014).
 - [11] S. Pirandola, R. Laurenza, C. Ottaviani, and L. Banchi, *Nat. Commun.* **8**, 15043 (2017).
 - [12] H.-J. Briegel, W. Dür, J. I. Cirac, and P. Zoller, *Phys. Rev. Lett.* **81**, 5932 (1998).
 - [13] L. Jiang, J. M. Taylor, K. Nemoto, W. J. Munro, R. Van Meter, and M. D. Lukin, *Phys. Rev. A* **79**, 032325 (2009).
 - [14] W. J. Munro, A. M. Stephens, S. J. Devitt, K. A. Harrison, and K. Nemoto, *Nat. Photonics* **6**, 777 (2012).
 - [15] S. Muralidharan, J. Kim, N. Lütkenhaus, M. D. Lukin, and L. Jiang, *Phys. Rev. Lett.* **112**, 250501 (2014).
 - [16] Z. Leghtas, G. Kirchmair, B. Vlastakis, R. J. Schoelkopf, M. H. Devoret, and M. Mirrahimi, *Phys. Rev. Lett.* **111**, 120501 (2013).
 - [17] M. Mirrahimi, Z. Leghtas, V. V. Albert, S. Touzard, R. J. Schoelkopf, L. Jiang, and M. H. Devoret, *New J. Phys.* **16**, 045014 (2014).
 - [18] D. Gottesman, A. Kitaev, and J. Preskill, *Phys. Rev. A* **64**, 012310 (2001).
 - [19] M. H. Michael, M. Silveri, R. T. Brierley, V. V. Albert, J. Salmilehto, L. Jiang, and S. M. Girvin, *Phys. Rev. X* **6**, 031006 (2016).
 - [20] S. Krastanov, V. V. Albert, C. Shen, C.-L. Zou, R. W. Heeres, B. Vlastakis, R. J. Schoelkopf, and L. Jiang, *Phys. Rev. A* **92**, 040303 (2015).
 - [21] R. W. Heeres, B. Vlastakis, E. Holland, S. Krastanov, V. V. Albert, L. Frunzio, L. Jiang, and R. J. Schoelkopf, *Phys. Rev. Lett.* **115**, 137002 (2015).
 - [22] R. W. Heeres, P. Reinhold, N. Ofek, L. Frunzio, L. Jiang, M. H. Devoret, and R. J. Schoelkopf, *arXiv:1608.02430 [Nat. Commun. (to be published)]*.
 - [23] K. W. Murch, S. J. Weber, C. Macklin, and I. Siddiqi, *Nature (London)* **502**, 211 (2013).
 - [24] M. Hatridge, S. Shankar, M. Mirrahimi, F. Schackert, K. Geerlings, T. Brecht, K. M. Sliwa, B. Abdo, L. Frunzio, S. M. Girvin, R. J. Schoelkopf, and M. H. Devoret, *Science* **339**, 178 (2013).
 - [25] L. Sun, A. Petrenko, Z. Leghtas, B. Vlastakis, G. Kirchmair, K. M. Sliwa, A. Narla, M. Hatridge, S. Shankar, J. Blumoff, L. Frunzio, M. Mirrahimi, M. H. Devoret, and R. J. Schoelkopf, *Nature (London)* **511**, 444 (2014).
 - [26] N. Ofek, A. Petrenko, R. Heeres, P. Reinhold, Z. Leghtas, B. Vlastakis, Y. Liu, L. Frunzio, S. M. Girvin, L. Jiang, M. Mirrahimi, M. H. Devoret, and R. J. Schoelkopf, *Nature (London)* **536**, 441 (2016).
 - [27] V. V. Albert and L. Jiang, *Phys. Rev. A* **89**, 022118 (2014).
 - [28] V. V. Albert, C. Shu, S. Krastanov, C. Shen, R.-B. Liu, Z.-B. Yang, R. J. Schoelkopf, M. Mirrahimi, M. H. Devoret, and L. Jiang, *Phys. Rev. Lett.* **116**, 140502 (2016).
 - [29] See Supplemental Material at <http://link.aps.org/supplemental/10.1103/PhysRevLett.119.030502> for the analysis of logical errors, quantification of error suppression, and repetitive correction with cat codes, which includes Refs. [30–34].
 - [30] V. Scarani, H. Bechmann-Pasquinucci, N. J. Cerf, M. Dušek, N. Lütkenhaus, and M. Peev, *Rev. Mod. Phys.* **81**, 1301 (2009).
 - [31] H.-K. Lau and M. B. Plenio, *Phys. Rev. Lett.* **117**, 100501 (2016).
 - [32] B. Mischuck and K. Molmer, *Phys. Rev. A* **87**, 022341 (2013).
 - [33] C. Axline, M. Reagor, R. Heeres, P. Reinhold, C. Wang, K. Shain, W. Pfaff, Y. Chu, L. Frunzio, and R. J. Schoelkopf, *Appl. Phys. Lett.* **109**, 042601 (2016).
 - [34] X.-B. Wang, *Phys. Rev. A* **71**, 052328 (2005).
 - [35] The backaction also corresponds to the subtle bias from the likelihood estimate of the logical states after the \mathbb{Z}_d measurement.
 - [36] C. Wang, Y. Y. Gao, P. Reinhold, R. W. Heeres, N. Ofek, K. Chou, C. Axline, M. Reagor, J. Blumoff, K. M. Sliwa, L. Frunzio, S. M. Girvin, L. Jiang, M. Mirrahimi, M. H. Devoret, and R. J. Schoelkopf, *Science* **352**, 1087 (2016).

- [37] N. Khaneja, T. Reiss, C. Kehlet, T. Schulte-Herbrüggen, and S. J. Glaser, *J. Magn. Reson.* **172**, 296 (2005).
- [38] Z. Leghtas, S. Touzard, I. M. Pop, A. Kou, B. Vlastakis, A. Petrenko, K. M. Sliwa, A. Narla, S. Shankar, M. J. Hatridge, M. Reagor, L. Frunzio, R. J. Schoelkopf, M. Mirrahimi, and M. H. Devoret, *Science* **347**, 853 (2015).
- [39] S. Lloyd and L. Viola, *Phys. Rev. A* **65**, 010101 (2001).
- [40] C. Shen, K. Noh, V. V. Albert, S. Krastanov, M. H. Devoret, R. J. Schoelkopf, S. M. Girvin, and L. Jiang, *Phys. Rev. B* **95**, 134501 (2017).
- [41] A. Kitaev, A. Shen, and M. Vyalı, *Classical and Quantum Computation* (American Mathematical Society, Providence, 2002).
- [42] G. Benenti and G. Strini, *J. Phys. B* **43**, 215508 (2010).
- [43] A. G. Fowler, D. S. Wang, C. D. Hill, T. D. Ladd, R. Van Meter, and L. C. L. Hollenberg, *Phys. Rev. Lett.* **104**, 180503 (2010).
- [44] W. J. Munro, K. Azuma, K. Tamaki, and K. Nemoto, *IEEE J. Sel. Top. Quantum Electron.* **21**, 78 (2015).
- [45] S. Muralidharan, C.-L. Zou, L. Li, J. Wen, and L. Jiang, *New J. Phys.* **19**, 013026 (2017).
- [46] S. Muralidharan, L. Li, J. Kim, N. Lütkenhaus, M. D. Lukin, and L. Jiang, *Sci. Rep.* **6**, 20463 (2016).
- [47] R. Namiki, L. Jiang, J. Kim, and N. Lütkenhaus, *Phys. Rev. A* **94**, 052304 (2016).
- [48] H. Paik, D. I. Schuster, L. S. Bishop, G. Kirchmair, G. Catelani, A. P. Sears, B. R. Johnson, M. J. Reagor, L. Frunzio, L. I. Glazman, S. M. Girvin, M. H. Devoret, and R. J. Schoelkopf, *Phys. Rev. Lett.* **107**, 240501 (2011).
- [49] R. Barends, J. Kelly, A. Megrant, D. Sank, E. Jeffrey, Y. Chen, Y. Yin, B. Chiaro, J. Mutus, C. Neill, P. O'Malley, P. Roushan, J. Wenner, T. C. White, A. N. Cleland, and J. M. Martinis, *Phys. Rev. Lett.* **111**, 080502 (2013).
- [50] J. M. Martinis and A. Megrant, [arXiv:1410.5793](https://arxiv.org/abs/1410.5793).
- [51] M. Hofheinz, H. Wang, M. Ansmann, R. C. Bialczak, E. Lucero, M. Neeley, A. D. O'Connell, D. Sank, J. Wenner, J. M. Martinis, and A. N. Cleland, *Nature (London)* **459**, 546 (2009).
- [52] J. Ghosh, A. Galiutdinov, Z. Zhou, A. N. Korotkov, J. M. Martinis, and M. R. Geller, *Phys. Rev. A* **87**, 022309 (2013).
- [53] B. M. Terhal and D. Weigand, *Phys. Rev. A* **93**, 012315 (2016).
- [54] K. Duivenvoorden, B. M. Terhal, and D. Weigand, *Phys. Rev. A* **95**, 012305 (2017).
- [55] J. Harrington and J. Preskill, *Phys. Rev. A* **64**, 062301 (2001).
- [56] A. Roy, A. D. Stone, and L. Jiang, *Phys. Rev. A* **94**, 032333 (2016).
- [57] B. Vermersch, P.-O. Guimond, H. Pichler, and P. Zoller, *Phys. Rev. Lett.* **118**, 133601 (2017).
- [58] Z.-L. Xiang, M. Zhang, L. Jiang, and P. Rabl, *Phys. Rev. X* **7**, 011035 (2017).
- [59] T. G. Tiecke, K. P. Nayak, J. D. Thompson, T. Peyronel, N. P. de Leon, V. Vuletić, and M. D. Lukin, *Optica* **2**, 70 (2015).
- [60] R. W. Andrews, R. W. Peterson, T. P. Purdy, K. Cicak, R. W. Simmonds, C. A. Regal, and K. W. Lehnert, *Nat. Phys.* **10**, 321 (2014).
- [61] C. O'Brien, N. Lauk, S. Blum, G. Morigi, and M. Fleischhauer, *Phys. Rev. Lett.* **113**, 063603 (2014).
- [62] C.-L. Zou, X. Han, L. Jiang, and H. X. Tang, *Phys. Rev. A* **94**, 013812 (2016).
- [63] M. Bergmann and P. van Loock, *Phys. Rev. A* **94**, 042332 (2016).